

Generation of highly entangled photon pairs for continuous variable Bell inequality violation

LIJIAN ZHANG[†], ALFRED B. U'REN^{*‡}, REINHARD ERDMANN[§],
KEVIN A. O'DONNELL[‡], CHRISTINE SILBERHORN[¶],
KONRAD BANASZEK^{||} and IAN A. WALMSLEY[†]

[†]Clarendon Laboratory, Oxford University, Parks Road, Oxford,
OX1 3PU, UK

[‡]Centro de Investigación Científica y Educación Superior de Ensenada (CICESE),
Ensenada, Baja California, 22860, Mexico

[§]Sensors Directorate, Air Force Research Laboratory, Rome, NY

[¶]Institut für Optik, Information und Photonik Universität Erlangen-Nürnberg,
91058 Erlangen, Germany

^{||}Institute of Physics, Nicolaus Copernicus University, ul. Grudziadzka 5,
PL-87-100 Toruń, Poland

(Received 20 January 2006)

We propose a novel experimental technique based on the process of parametric downconversion for the generation of photon pairs characterized by ultra-high dimensional spectral entanglement. It is shown that a superlattice of nonlinear and linear segments can be exploited to obtain states exhibiting a remarkably large entanglement, with a Schmidt number in the region of 10^7 . We furthermore consider the application of such highly entangled photon pairs for the violation of a Bell inequality constructed from a measurement of the transverse wavevector Wigner function; such an approach eliminates the need for filtering the photon pairs and consequently eliminates an important potential loophole.

1. Introduction

Entanglement is the essential feature which differentiates quantum from classical systems and has been the core ingredient in many recent experiments and proposals designed to test the validity of quantum mechanics and to develop quantum-enhanced technologies. Continuous variable bi-partite quantum systems present the possibility of dramatically larger entanglement (as quantified for example by the Schmidt number) compared to systems described by low-dimensional Hilbert spaces such as those based on spin. An important physical system exhibiting both kinds of structure is that of photon pairs. Here polarization plays the role of spin, and the transverse and longitudinal degree of freedom are continuous.

*Corresponding author. Email: auren@cicese.mx

While idealized polarization-entangled photon pairs have a Schmidt number of 2, photon pairs exhibiting entanglement in a continuous degree of freedom, such as frequency or transverse wavevector, have in principle no upper limit to the attainable Schmidt number [1]. In this paper we explore the generation of photon pairs characterized by a particularly large Schmidt number, generated by the process of parametric downconversion (PDC) in specific geometries. Such states constitute extreme examples of light characterized by non-classical properties and have a number of exciting applications, apart from fundamental interest in the study of high-dimensional entanglement. They have, for example, been shown to lead to a particularly large flux of photon pairs retaining a measurable non-classical character [2]; likewise they have been shown to lead to the shortest possible time of emission difference distributions between signal and idler, useful for metrology [3]. As described in [4], such states furthermore lead to a drastically boosted mutual information between the signal and idler modes, which leads to quantum communication and cryptography protocols exploiting the richness of the continuous degrees of freedom to enhance the information transmission capacity. In this paper we present a specific experimental technique designed to yield photon pairs with an ultra large Schmidt number at essentially arbitrary PDC wavelengths. We likewise show that such highly entangled photon pairs can yield the violation of a continuous variable Bell inequality without recourse to projective measurements to a subspace of the full Hilbert space, thus closing a potentially important loophole in the validation of quantum mechanics versus local realism.

In general, PDC photon pairs exhibit complicated correlations between the spatial and spectral degrees of freedom, as a consequence of the fact that the energy and momentum conservation constraints are not independent of each other due to dispersion in the nonlinear medium. In practice narrowband filters (spectral or spatial) are often used to restrict attention to one degree of freedom or another in order to bring out the general characteristics of the entanglement in each particular case of interest. As interest grows in states exhibiting more complicated entanglement involving more than one degree of freedom (sometimes referred to as hyper-entanglement), it will become important to consider spectral and spatial correlations simultaneously. In this paper, however, we restrict attention to one degree of freedom at a time. While in section 2 we deal with states characterized by very large spectral entanglement; in section 3 we consider states highly entangled in the spatial degree of freedom.

2. Two photon state engineering via crystal sequences with linear compensators

In this section we focus on the generation of photon pair states exhibiting ultra-high dimensional entanglement in the spectral (temporal) degree of freedom. It will be shown that the use of type-I phasematched PDC coupled with the use of a quasi-monochromatic pump can result in highly entangled photon pairs in the spectral degree of freedom. It will be shown, additionally, that by employing a superlattice of nonlinear and linear crystals chosen so as to eliminate the overall group velocity dispersion, the Schmidt number can be enhanced further.

In order to describe PDC states generated by a quasi-monochromatic pump, it is convenient to define the frequency variables $\nu_{\pm} = 2^{-1/2}(\nu_s \pm \nu_i)$ in terms of the signal (s) and idler (i) frequency detunings $\nu_{\mu} = \omega_{\mu} - \omega_0$ (where $\mu = s, i$) from the degenerate PDC frequency ω_0 . It can be shown that the PDC state can then be expressed as

$$|\Psi\rangle = A \iint d\nu_+ d\nu_- \alpha(\nu_+) \phi_-(\nu_-) |2^{-1/2}(\nu_+ + \nu_-)\rangle_s |2^{-1/2}(\nu_+ - \nu_-)\rangle_i, \quad (1)$$

where A is a normalization constant and $|\dots\rangle_{\mu}$ (with $\mu = s, i$) represents single photon Fock states in the signal and idler modes. $\alpha(\nu_+) \phi_-(\nu_-)$ (see equation (1)) represents the joint spectral amplitude given in terms of the pump envelope function (PEF) $\alpha(\nu_+)$ and a one-dimensional phasematching function (PMF) $\phi_-(\nu_-)$ defined in terms of the full PMF $\phi(\nu_+, \nu_-) = \text{sinc}[\Delta k(\nu_+, \nu_-)L/2]$ (where $\Delta k(\nu_+, \nu_-)$ denotes the phasemismatch and L is the crystal length) by

$$\phi_-(\nu_-) = \lim_{\nu_+ \rightarrow 0} \phi(\nu_+, \nu_-). \quad (2)$$

Let us note that the spectral width along ν_+ is determined by the pump bandwidth which for a quasi-monochromatic pump (e.g. in the MHz range) is typically orders of magnitude smaller than the width of the PMF along ν_+ .

The cooperativity parameter (also known as the Schmidt number) K is a convenient quantifier of the effective dimensionality of the Hilbert space describing the continuous variable structure of the PDC photon pairs. Following the arguments in [5], if each of $\alpha(\nu_+)$ and $\phi_-(\nu_-)$ are described by Gaussian functions with widths σ_+ and σ_- respectively, it is possible to obtain an analytic expression for K . In the limit where $\sigma_+ \ll \sigma_-$, we obtain the expression $K = \sigma_-/2^{1/2}\sigma_+$. Thus, it becomes clear that in order to obtain highly entangled states of the kind discussed above, we require the narrowest possible pump bandwidth (which determines σ_+) and the widest possible PDC bandwidth, quantified by σ_- . In what follows we develop a specific technique designed to enhance the PDC bandwidth [6] while employing a particularly narrow pump bandwidth. We will show that σ_-/σ_+ ratios of $\sim 10^7$ are possible, representing states with an extraordinarily high dimensional entanglement in the spectral degree of freedom.

We exploit nonlinear crystal superlattices [7], where the dispersion exhibited by thin crystal segments is compensated for by that in appropriately chosen linear optical media. Such a technique has proven powerful for the generation of a variety of states including those optimized for Hong–Ou–Mandel interferometry [8], those characterized by spectral decorrelation crucial for the successful concatenation of multiple heralded single photon sources [9] and time-bin qudits [10]. While in the cases described above, it suffices to consider group velocity crystal dispersion terms, high dimensional entangled states can be enhanced by control over group velocity dispersion (GVD) terms; specifically, as will be shown below, when the GVD coefficient at the degenerate PDC wavelength vanishes, the PDC spectrum can be significantly broadened. Specific materials meet this condition only at certain wavelengths, thus limiting the usefulness of such an approach. We will show, however, that through the use of crystal superlattices, the overall GVD term can be made to vanish provided a certain condition (see below) is met by the superlattice materials.

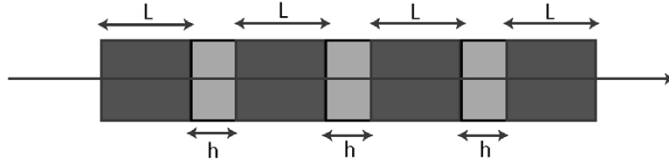


Figure 1. Sequence comprised of N $\chi^{(2)}$ crystals interspersed with $N-1$ birefringent spacers.

A source engineered in this way dramatically enhances the range of wavelengths at which it is possible to obtain two photon states characterized by particularly high dimensional entanglement.

Consider the arrangement shown in figure 1 consisting of N identical $\chi^{(2)}$ crystals and $N-1$ linear optical $\chi^{(1)}$ spacers. Each of the crystals is assumed to be cut and oriented for degenerate collinear type-I PDC while the compensators are assumed not to exhibit a $\chi^{(2)}$ nonlinearity. It is further assumed that each crystal has length L while each spacer has length h . The phase mismatch in each of the crystals is given by

$$\Delta k = k_s + k_i - k_p, \quad (3)$$

where k_μ (with $\mu = p, s, i$) denotes the wavenumber for each of the three fields taking into account dispersion in the crystal. The phase mismatch introduced by each of the spacers is equivalently given by

$$\Delta \kappa = \kappa_s + \kappa_i - \kappa_p, \quad (4)$$

where κ_μ (with $\mu = p, s, i$) now represents the wavenumber for each of the three fields taking into account dispersion in the birefringent spacer. For an assembly of N crystals and $N-1$ spacers the overall phasematching function can then be calculated as

$$\begin{aligned} \phi_N(\Delta k, \Delta \kappa) &= \sum_{m=0}^{N-1} \exp[im(L\Delta k + h\Delta \kappa)] \operatorname{sinc} \left[\frac{L}{2} \Delta k \right] \\ &\propto \exp \left\{ \frac{i}{2} [N\Delta k(v_s, v_i)L + (N-1)\Delta \kappa(v_s, v_i)h] \right\} \Upsilon_N \left[\frac{\Phi}{2} \right] \operatorname{sinc} \left[\frac{L\Delta k}{2} \right], \end{aligned} \quad (5)$$

where we have defined the quantity Φ as

$$\Phi = L\Delta k + h\Delta \kappa \quad (6)$$

and where

$$\Upsilon_N(x) = \frac{1}{N} \frac{\sin(Nx)}{\sin(x)}. \quad (7)$$

Hence, apart from an overall phase factor the crystal assembly phasematching function is composed of the product of two distinct functions: one corresponds to the

phasematching function of a single crystal and the second factor incorporates the combined effect of the crystal and spacer dispersion. In order to carry out more explicit calculations, it is helpful to write down the crystal and spacer phase mismatch as a Taylor expansion where we omit all terms of higher order than quartic in ν . Thus, we obtain, in terms of the frequency variables ν_{\pm} :

$$\begin{aligned} \Phi = & L\Delta k^{(0)} + h\Delta\kappa^{(0)} + 2^{1/2}Tv_+ + B(\nu_+^2 + \nu_-^2) - B_p\nu_+^2 \\ & + C(3\nu_-^2\nu_+ + \nu_+^3) - C_p\nu_+^3 \\ & + D(\nu_-^4 + 6\nu_+^2\nu_-^2 + \nu_+^4) - D_p\nu_+^4 + \vartheta(\nu^5), \end{aligned} \quad (8)$$

where $L\Delta k^{(0)}$ and $h\Delta\kappa^{(0)}$ denote the constant terms of the Taylor expansions and where T, B, B_p, C, C_p, D and D_p denote the coefficients of the linear, quadratic, cubic and quartic expansion terms and where $\vartheta(\nu^5)$ denotes quintic and higher order terms.

We now impose the condition

$$h = \frac{2\pi m}{2\kappa(\omega_0) - \kappa_p(2\omega_0)}, \quad (9)$$

where m is any integer which guarantees a vanishing constant term due to the superlattice. We furthermore assume that $\Delta k^{(0)} = 0$ as required for each crystal segment to exhibit phasematching.

The joint spectral amplitude is then given by the product of the phasematching function and the pump envelope function, as in equation (1). In the limit of a quasi-monochromatic pump (see equation (2)) odd order dispersion terms in Φ drop out; we thus obtain

$$\phi_-(\nu_-)\alpha(\nu_+) = \Upsilon_N[(B\nu_-^2 + D\nu_-^4)/2] \text{sinc}(\beta\nu_-^2/2) \exp(-2\nu_+^2/\sigma^2) \quad (10)$$

in terms of two GVD coefficients:

$$B = \frac{1}{2}[Lk''(\omega_0) + h\kappa''(\omega_0)], \quad (11)$$

$$\beta = \frac{L}{2}k''(\omega_0) \quad (12)$$

and a quartic dispersion coefficient

$$D = \frac{1}{48}[Lk^{(4)}(\omega_0) + h\kappa^{(4)}(\omega_0)], \quad (13)$$

where $''$ denotes a second derivative and $^{(4)}$ denotes a fourth derivative. In order to gain physical insight, let us first consider the case $h=0$, i.e. the case where the superlattice reduces to a continuous crystal of length $\ell = NL$. In this case, the joint spectral amplitude becomes

$$\phi_-(\nu_-)\alpha(\nu_+) = \text{sinc}[\beta'\nu_-^2/2 + \vartheta(\nu^4)] \exp(-2\nu_+^2/\sigma^2) \quad (14)$$

with $\beta' = \ell k''(\omega_0)/2$. Let us note that the PDC spectral width is determined by the GVD coefficient β' ; it is clear that if β' is made to vanish, the width is now determined by a quartic dispersion coefficient, typically leading to a drastically boosted PDC bandwidth. As has been discussed above, the condition $\beta' = 0$ occurs for some

materials at specific wavelengths. Here we show, however, that through the use of a superlattice the overall GVD coefficient B (see equation (11)) can be made to vanish at arbitrary wavelengths independently of the underlying crystal dispersion, which can result in high dimensional entangled states at arbitrary wavelengths if short crystal segments are used.

Thus, the technique presented here relies on imposing the condition $B=0$ so that the lowest order term in the argument of the Υ_N function is quartic in ν_- . Note that for this to be possible: (i) $k''(\omega_0)$ and $\kappa''(\omega_0)$ must exhibit opposite signs and (ii) the thicknesses L and h must be chosen such that the overall GVD coefficient B vanishes. If, in addition, short crystal segments are employed, the superlattice contribution dominates over the single-crystal contribution in equation (10). Note that in this case the dominant term is quartic and proportional to parameter D , which for typical crystals is small resulting in an extraordinarily broad joint spectral intensity along ν_- . Note that along ν_+ the joint spectral profile is determined by the pump bandwidth, which we are here assuming to be extremely small (in the region of MHz).

For concreteness, let us consider a specific example. Consider the use of lithium niobate (PPLN) crystal segments periodically poled for degenerate type-I PDC centred at $1.55\ \mu\text{m}$, a useful wavelength for fibre communications. We assume all three fields to be ‘e’ waves and a quasi-phasematching periodicity of $18.7\ \mu\text{m}$. In addition, let us consider calcite spacers aligned so that the signal and idler photons experience the ordinary index of refraction. It turns out that while for the PPLN segments $k''(\omega_0) = 1.0 \times 10^{-31}\ \text{s}^2\ \mu\text{m}^{-1}$, for the calcite segments $\kappa''(\omega_0) = -2.1 \times 10^{-32}\ \text{s}^2\ \mu\text{m}^{-1}$. Thus, the calcite thickness h to PPLN thickness L ratio must be ≈ 4.9 to guarantee that the overall GVD term B vanishes. In the plots below we assume $h = 487\ \mu\text{m}$ (corresponding to $m=10$ in equation (9)) and $L = 100\ \mu\text{m}$; we assume a superlattice comprised of 10 nonlinear crystals and 9 linear spacers. We furthermore assume a quasi-monochromatic pump with 5 MHz bandwidth. Figure 2 shows the resulting joint spectral intensity. Given the extremely high aspect ratio of the resulting two-photon state, for graphical clarity we plot diagonal slices along the directions $\omega_s + \omega_i$ and $\omega_s - \omega_i$. Thus, figure 2(a) shows the joint spectral intensity evaluated at $\omega_i = 2\omega_0 - \omega_s$ and plotted as a function of wavelength in μm ; the solid line results from the superlattice described above while the dashed line represents the case of a continuous PPLN crystal of length equivalent to 10 crystal segments (as can be seen, the superlattice results in approximately a threefold increase in PDC bandwidth). Figure 2(b) shows the joint spectral intensity evaluated at $\omega_s = \omega_i$ as a function of frequency in MHz. Note that along ω_- the signal extends roughly from 1.25 to $2\ \mu\text{m}$, which represents an extraordinarily large bandwidth. At the same time, the bandwidth along the $\omega_s + \omega_i$ is some 7 orders of magnitude smaller (5 MHz versus ~ 90 THz), which translates into a state with exceptionally large spectral entanglement.

The very large information content in a two-photon state of the sort described here is unfortunately not easily accessible. The information resides in the spectral and temporal entanglement of the two photons—that is in their negative frequency correlation and their positive temporal correlation. To make use of this requires nonstationary optical elements, such as shutters, phase modulators or detectors

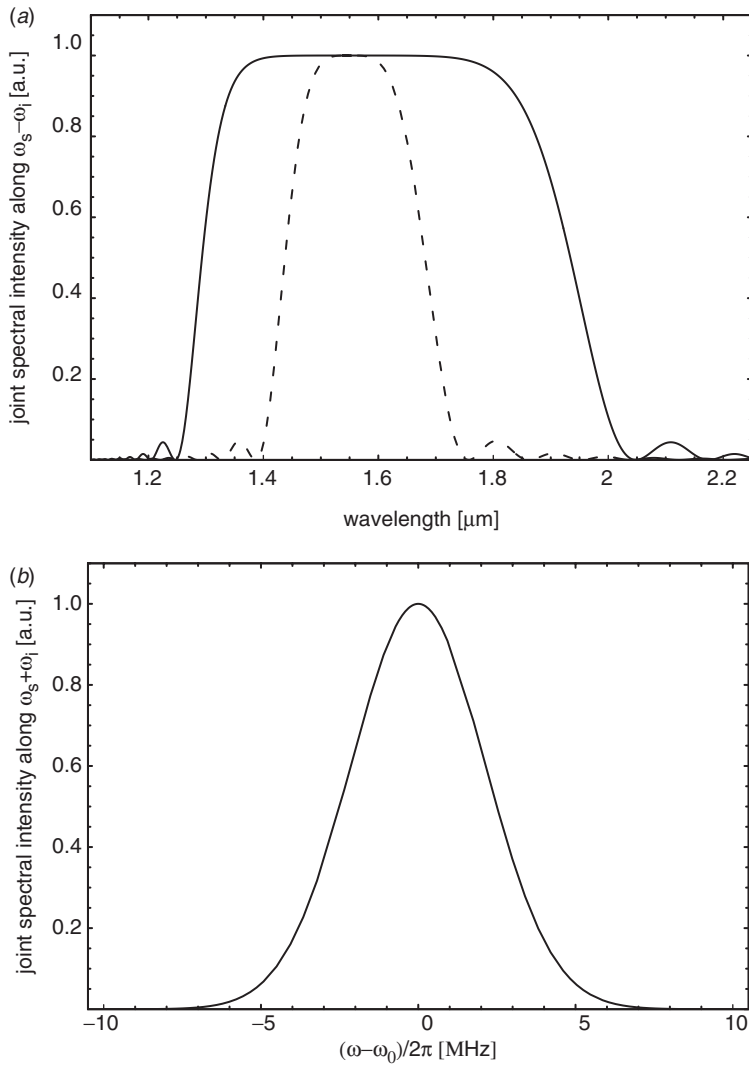


Figure 2. (a) Slice along ω_- of the joint spectral intensity for superlattice (solid line) and for equivalent continuous crystal (dashed line). (b) Slice along ω_+ of the joint spectral intensity. Notice the extremely high ratio of the two bandwidths, resulting in an exceptionally large spectral entanglement.

whose response time is comparable to the correlation time between the two photons (i.e. to the width of the signal-idler time of emission difference distribution), which for the state in figure 2 is in the order of a few femtoseconds. Such components do not exist at present. Similarly, very high spectral resolution, on the order of the pump bandwidth is also required. If such devices are available then slow detectors may in principle be used, the number of which is equal to the number of bits of mutual information between the pair of photons.

Massive entanglement of this kind has also been discussed for the spatial domain, for which elements with high spatial and angular resolution are available [1, 11, 12]. This therefore seems a more plausible approach. Unfortunately, the number of Schmidt modes that is realistically accessible is limited by the extent of the optical imaging system and the dimensions of the nonlinear media and pump beam to be substantially smaller than the $\sim 10^7$ available in the spectral case.

In conclusion, we have presented a novel technique based on a superlattice of nonlinear crystals and linear compensators coupled with the use of a quasi-monochromatic pump which can yield states, centred at arbitrary wavelengths, characterized by extraordinarily high dimensional entanglement in the spectral degree of freedom. It is expected that this work will facilitate the further exploration of highly entangled quantum systems.

3. Violation of a continuous variable Bell inequality based on the spatial Wigner function

The nonclassical character of entangled states of particles with a 2-dimensional Hilbert space are well understood and are the basis for numerous applications. However, the non-classical features of this kind of state in continuous spaces have not attracted much attention. In this section, we show that highly entangled states can be used to test the nonlocality of quantum theory by violating Bell inequalities. For the convenience of experiment, we consider the spatial structures of the PDC photons generated by bulk crystals.

Bell inequalities provide one measure of the nonclassicality of a composite quantum system, by testing whether a local realistic model can describe the results of measurements on the system. The original Bell inequality relies on dichotomic outcomes of measurements on each of the subsystems [13, 14]. Recently there have been discussions on the generalization of Bell inequalities to N -value observables with $N \geq 3$ [15–17]. When N increases this requires large detector arrays, which makes it challenging for experimental realizations. In this section we restrict our attention to the Bell inequalities based on dichotomous observables. Therefore it is necessary to identify a way in which a given state may yield only two possible results for the specified measurement.

The first Bell inequality violation was shown with a singlet state of two spin-1/2 particles [13, 18]. Since then, it has been considered whether it is possible to violate the Bell inequality using the original, continuous-variable entangled EPR state [19] with the wave function

$$\psi(x_1, x_2) = \int_{-\infty}^{\infty} \exp[(2\pi i/h)(x_1 - x_2 + x_0)p] dp. \quad (15)$$

Although this state has some mathematical problems due to its singularity, it can be regarded as the limit of an appropriate class of smoothed normalizable states [20] to overcome this difficulty. Since an arbitrary system can be separated into dichotomous observables, these realistic states can be used to demonstrate violations of Bell inequalities. An easier approach is to operate on only one two-dimensional

subspace, and discard the photons that do not fall into it. For example, Cohen [20] shows that a Bell state can be produced by selecting two pairs of correlated space–time modes from the continuum occupied by each EPR particle. This allows the momentum-entangled photons to be treated exactly like polarization-entangled photons. However, this procedure works by throwing away nearly all the amplitude of the EPR state, creating a spin-like state by projecting onto a dichotomic subspace of the original, continuous Hilbert space. This idea was, in fact, the basis for a practical realization by Tapster and Rarity of Bell inequality violations using frequency and momentum entanglement of photon pairs [21]. In these experiments, pinholes were used to select just two pairs of correlated modes, thus discarding most of the correlated particles produced by the quantum source. This severely limits the signal-to-noise ratio of the experiments, and provides an obvious loophole.

Losses have proven to be a most difficult obstacle to any loophole free experiment that violates nonlocality. Therefore it would be a significant achievement to demonstrate that a Bell inequality is violated with continuous degrees of freedom, without discarding any of the photons used to provide the information. This can be done by measuring the joint Wigner function of the two-photon state. Although Bell argued that a positive definite Wigner function allows for a local hidden variable description of the correlations [22], it has been shown that the positivity or negativity of the Wigner function has a very weak relation to the locality problem [23]. In fact, it has been proven that the Wigner function is equivalent to the expectation value of the parity operators [24]. As the measurement of the parity operator only yields two values: +1 and –1, the Wigner function satisfies the condition for constructing Bell inequalities. Now let us examine the spatial degree of freedom of a two photon state (cf. equation (1), which considers only the frequency part)

$$|\psi\rangle = \int dk_1 dk_2 \psi(k_1, k_2) |k_1\rangle |k_2\rangle, \quad (16)$$

where $\psi(k_1, k_2)$ plays the role of a two-photon wavefunction [4]. The Wigner function is given by

$$W(x_1, k_1; x_2, k_2) = \frac{4}{\pi^2} \Pi(x_1, k_1; x_2, k_2), \quad (17)$$

where $\Pi(x_1, k_1; x_2, k_2)$ is the Wigner transform of the biphoton wavefunction:

$$\begin{aligned} \Pi(x_1, k_1; x_2, k_2) &= \int d\xi_1 d\xi_2 \exp(2ix_1\xi_1) \exp(2ix_2\xi_2) \psi^* \\ &\quad \times (k_1 - \xi_1, k_2 - \xi_2) \psi(k_1 + \xi_1, k_2 + \xi_2). \end{aligned} \quad (18)$$

Using the method in [14], we can construct the combination

$$B = \Pi(0, 0; 0, 0) + \Pi(J^{1/2}, 0; 0, 0) + \Pi(0, 0; -J^{1/2}, 0) - \Pi(J^{1/2}, 0; -J^{1/2}, 0), \quad (19)$$

where $J^{1/2}$ characterizes the magnitude of the displacement. For local hidden variable (LHV) theories, B should satisfy the inequality $-2 \leq B \leq 2$.

For degenerate PDC with collinear phase matching in a bulk crystal, the joint probability amplitude of the two photon state has a expression similar to equation (1) [25]

$$\psi(k_1, k_2) \propto \exp\left[-\frac{w_0^2}{4}(k_1 + k_2)^2\right] \text{sinc}\left[\frac{L}{4k_p}(k_1 - k_2)^2\right], \quad (20)$$

where w_0 is the spot size of the pump, L is the length of the nonlinear crystal and k_p is the wave vector of the pump. We should indicate that in contrast to Gaussian-correlated states [20], the PDC state has negative values for the Wigner function at some points. From equations (18), (19) and (20), we can calculate B for the entangled photon state. Similar to the Schmidt number K , the maximum value of B is determined by $k_p^{1/2}w_0/L^{1/2}$, which plays a similar role to σ_-/σ_+ in section 2. By selecting proper configurations, Bell inequalities can be violated. Figure 3(a) shows the relation between B_{\max} and $k_p^{1/2}w_0/L^{1/2}$ for the Gaussian correlated state with the same parameters as the PDC state in equation (20)†

$$\psi(k_1, k_2) \propto \exp\left[-\frac{w_0^2}{4}(k_1 + k_2)^2\right] \exp\left[-\frac{L}{4k_p}(k_1 - k_2)^2\right]. \quad (21)$$

Although there is entanglement between the two photons when $k_p^{1/2}w_0/L^{1/2} < 1$, the combination in equation (19) will not violate the Bell inequality. When $k_p^{1/2}w_0/L^{1/2} \geq 1$, B_{\max} increases with $k_p^{1/2}w_0/L^{1/2}$ and approaches its limit 2.19. Figure 3(b) shows the calculated B for a realistic PDC source with $L=3$ mm, $w_0=2$ mm and a monochromatic pump at 400 nm. For this configuration, when $|J^{1/2}| < 2.5$ μm , the Bell inequality is violated.

Therefore it is possible to violate the Bell inequality using the correlations of continuous spatial variables of a realistic PDC source without discarding any photons. Rather than manipulating the input state using a projection in order to obtain a Bell state, we instead construct a dichotomic observable that is non-zero for any biphoton state. Furthermore the use of the spatial degree of freedom of the entangled photon pairs overcomes one of the main obstacles for realizations of CV entanglement in field quadratures [23, 26]: the degradation of the quantum correlations due to inevitable, optical losses and inefficiencies in real systems. Experiments using photon pairs are not hampered by losses, since the photon number is decoupled from the observed correlated variables such that viable results can be post-selected.

Another advantage of using the Wigner function in real space is that it can be measured directly using Sagnac interferometers. The proposed experimental setup is shown in figure 4(a). The apparatus consists of two Sagnac interferometers shown in figure 4(b). Before entering each interferometer, the input photon is steered by a mirror (M1 in the figure). The displacement and tilt of the mirrors determine the point at which the Wigner function is measured [27]. Each interferometer includes an

† With the same parameters, the Schmidt numbers of the Gaussian correlated state and the PDC state will vary in a similar way, i.e. both of them meet the minimum value $k_p^{1/2}w_0/L^{1/2} = 1$ [1].

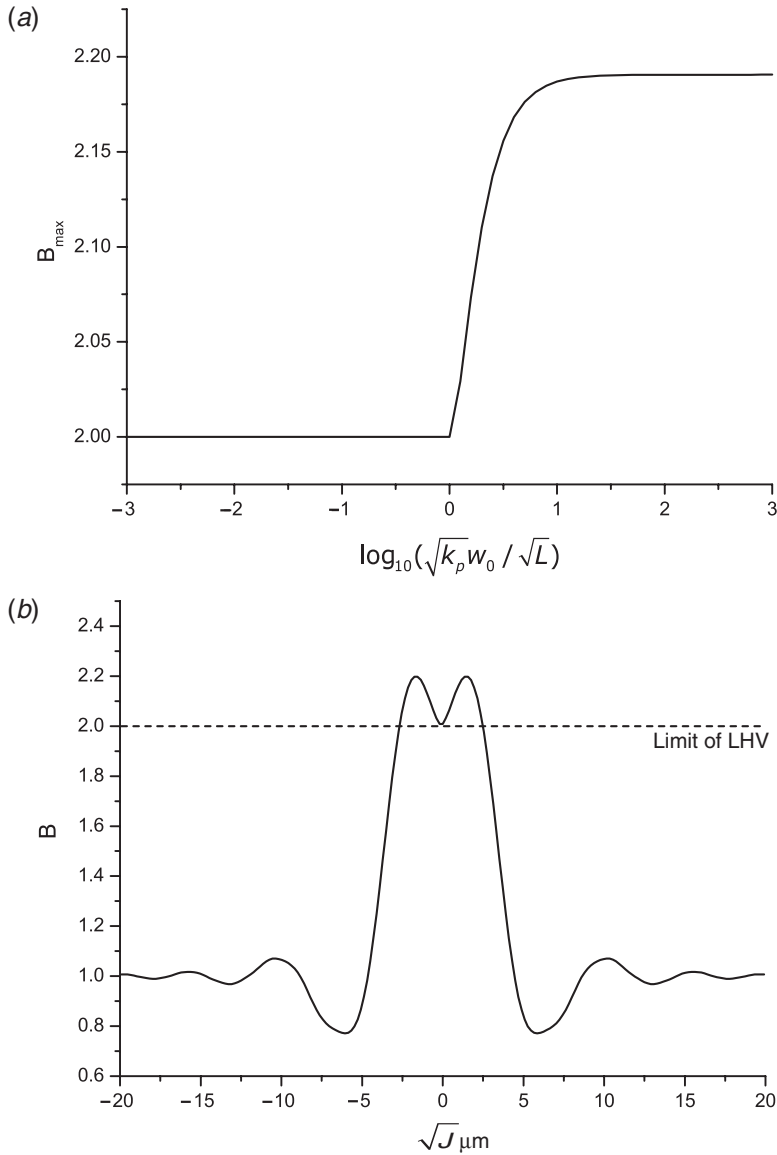


Figure 3. (a) The relation between B_{\max} and $k_p^{1/2}w_0/L^{1/2}$ for Gaussian correlated states. (b) Plot of the combination B for a realistic PDC source. The photons are generated in a 3 mm thick BBO crystal which is pumped by a monochromatic beam $\lambda = 400$ nm with a 2 mm spot size.

image rotator, which acts as the spatial inversion of the photon. Multiplying the difference signals from each of the interferometers recorded at coincident times gives the joint Wigner distribution for the two points in space. By selecting appropriate configurations of the PDC source and displacements of the mirrors, the results of

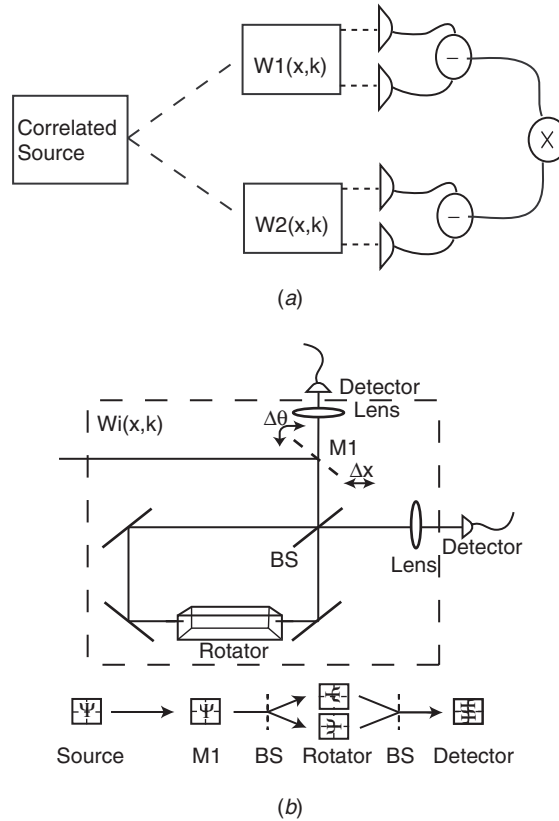


Figure 4. (a) Apparatus for measuring the spatial joint Wigner function of the PDC source. Each arm consists of a Sagnac interferometer shown in (b).

measurements will violate local realism. Nevertheless, there will likely be some restrictions on the possible states testable in this way due to the finite numerical aperture of the Sagnac interferometer. This would need more study before it can be properly claimed that the selection loophole can be closed in this way.

4. Conclusions

We have proposed a novel technique for the generation of highly entangled photon pairs, based on the use of a quasi-monochromatic pump together with the suppression of group velocity dispersion via a superlattice source comprised of adequately chosen linear and nonlinear segments. We have shown that this technique permits the synthesis of states characterized by extremely large spectral entanglement; we have furthermore shown that for realistic experimental parameters Schmidt numbers in the region of 10^7 are possible. Highly entangled states of this type enable a number of crucial applications. In particular, we have shown that a highly entangled state in

the spatial degree of freedom leads to the violation of a continuous variable Bell inequality based on the complete two-photon amplitude (without recourse to selection or filtering), thus in principle closing an important loophole.

References

- [1] C.K. Law and J.H. Eberly, *Phys. Rev. Lett.* **92** 127903 (2004).
- [2] B. Dayan, A. Pe'er, A.A. Friesem, *et al.*, *Phys. Rev. Lett.* **94** 043602 (2005).
- [3] D. Strelkalov, A.B. Matsko, A. Savchenkov, *et al.*, *J. Mod. Opt.* **52** 2233 (2005).
- [4] L. Zhang, A.B. U'Ren, Ch. Silberhorn, *et al.*, in *Continuous Variables in Quantum Optics*, edited by G. Leuchs and N. Cerf (World Scientific, Singapore, 2006).
- [5] A.B. U'Ren, K. Banaszek and I.A. Walmsley, *Quantum Informat. Comput.* **3** 480 (2003).
- [6] M.B. Nasr, G. Di Giuseppe, B.E.A. Saleh, *et al.*, *Opt. Commun.* **246** 521 (2005).
- [7] D.N. Klyshko, *JETP* **77** 222 (1993).
- [8] A.B. U'Ren, R. Erdmann, M. de la Cruz-Gutierrez, *et al.*, to be published (2006).
- [9] A.B. U'Ren, Ch. Silberhorn, K. Banaszek, *et al.*, *Laser Phys.* **15** 146 (2005).
- [10] A.B. U'Ren, R. Erdmann and I.A. Walmsley, *J. Mod. Opt.* **52** 2197 (2005).
- [11] M.N. O'Sullivan-Hale, I.A. Khan, R.W. Boyd, *et al.*, *Phys. Rev. Lett.* **94** 220501 (2005).
- [12] J.C. Howell, R.S. Bennink, S.J. Bentley, *et al.*, *Phys. Rev. Lett.* **92** 210403 (2004).
- [13] J.S. Bell, *Physics* (Long Island City, NY) **1** 195 (1964).
- [14] J.F. Clauser, M.A. Horne, A. Shimony, *et al.*, *Phys. Rev. Lett.* **23** 880 (1969).
- [15] D. Kaszlikowski, P. Gnaniński, M. Zukowski, *et al.*, *Phys. Rev. Lett.* **85** 4418 (2000).
- [16] D. Collins, N. Gisin, N. Linden, *et al.*, *Phys. Rev. Lett.* **88** 040404 (2002).
- [17] A. Vaziri, G. Weihs and A. Zeilinger, *Phys. Rev. Lett.* **89** 240401 (2002).
- [18] D. Bohm and Y. Aharonov, *Phys. Rev.* **108** 1070 (1957).
- [19] A. Einstein, B. Podolsky and N. Rosen, *Phys. Rev.* **47** 777 (1935).
- [20] O. Cohen, *Phys. Rev. A* **56** 3484 (1997).
- [21] J.G. Rarity and P.R. Tapster, *Phys. Rev. Lett.* **64** 2495 (1990).
- [22] J.S. Bell, *Speakable and Unspeakable in Quantum Mechanics* (Cambridge University Press, Cambridge, 1987), Chap. 21.
- [23] K. Banaszek and K. Wódkiewicz, *Phys. Rev. A* **58** 4345 (1998).
- [24] A. Royer, *Phys. Rev. A* **15** 449 (1977).
- [25] S.P. Walborne, A.N. de Oliveira, S. Pádua, *et al.*, *Phys. Rev. Lett.* **90** 143601 (2003).
- [26] K. Banaszek and K. Wódkiewicz, *Phys. Rev. Lett.* **82** 2009 (1999).
- [27] E. Mukamel, K. Banaszek, I.A. Walmsley, *et al.*, *Opt. Lett.* **28** 1317 (2003).